

## Article

# Uptake of Cationic PAMAM-PLGA Nanoparticles by the Nasal Mucosa

Mohammed A. Albarki <sup>1,2,\*</sup>  and Maureen D. Donovan <sup>2</sup><sup>1</sup> Pharmacy Department, Al-Mustaqbal University College, Babylon 51001, Iraq<sup>2</sup> Department of Pharmaceutics and Translational Therapeutics, College of Pharmacy, University of Iowa, Iowa City, IA 52242, USA

\* Correspondence: mohammed.albarki@uomus.edu.iq; Tel.: +964-780-657-5353

**Abstract:** Nanoparticles provide promising advantages in advanced delivery systems for enhanced drug delivery and targeting. The use of a biodegradable polymer such as PLGA (poly lactic-co-glycolic acid) promotes improved nanoparticle safety and, to some extent, provides the ability to modify nanoparticle surface properties. This study compared the effect of altering the surface charge on the translocation of PLGA nanoparticles across excised nasal mucosal tissues. Nanoparticles (average diameter of 60–100 nm) loaded with Nile Red (lipophilic fluorescent dye) were fabricated using a nanoprecipitation method. The effects of nanoparticle surface charge were investigated by comparing the transfer of untreated nanoparticles (negatively charged) and positively charged PLGA nanoparticles, which were modified using PAMAM dendrimer (polyamidoamine, 5th generation). All nanoparticles were able to be transferred in measurable quantities into both nasal respiratory and olfactory mucosae within 30 min. The total nanoparticle uptake was less than 5% of the nanoparticle mass exposed to the tissue surface. The cationic nanoparticles showed a significantly lower transfer into the mucosal tissues where the amount of nanoparticles transferred was 1.8–4-fold lower compared to the untreated negatively charged nanoparticles. The modification of the nanoparticle surface charge can alter the nanoparticle interaction with the nasal epithelial surface, which can result in decreasing the nanoparticle transfer into the nasal mucosa.

**Keywords:** PLGA nanoparticles; cationic nanoparticles; PAMAM dendrimer; intranasal; drug delivery; nanoprecipitation



**Citation:** Albarki, M.A.; Donovan, M.D. Uptake of Cationic PAMAM-PLGA Nanoparticles by the Nasal Mucosa. *Sci. Pharm.* **2022**, *90*, 72. <https://doi.org/10.3390/scipharm90040072>

Academic Editor:  
Natasa Skalko-Basnet

Received: 7 October 2022  
Accepted: 17 November 2022  
Published: 25 November 2022

**Publisher's Note:** MDPI stays neutral with regard to jurisdictional claims in published maps and institutional affiliations.



**Copyright:** © 2022 by the authors. Licensee MDPI, Basel, Switzerland. This article is an open access article distributed under the terms and conditions of the Creative Commons Attribution (CC BY) license (<https://creativecommons.org/licenses/by/4.0/>).

## 1. Introduction

Intranasal administration is considered a non-invasive route for systemic as well as for local drug delivery. In addition, it may enable drug administration to the CNS via nose-to-brain pathways [1,2]. Nanoparticle delivery systems are promising carriers that can improve drug targeting and treatment efficacy for challenging drugs [3]. Nanoparticles have been under investigation for many years for their applications as delivery systems owing to the capability to modify their characteristics, such as diameter and surface charge, and the ability to use relatively safe biodegradable polymers as the core material [4–7]. A nanoparticulate delivery system can be used to enhance drug targeting and minimize unwanted drug effects on biological systems. Biodegradable polymers, such as PLGA (poly-lactic-co-glycolic acid), have demonstrated good safety and ease of surface modification, which make these polymers a desirable choice as a core material in nanoparticle preparations.

Nanoparticle immunogenicity and translocation across body barriers are subjected to alteration based on the charge presented on the nanoparticle surface. Cationic nanoparticles were reported to have significantly higher uptake in comparison to unmodified nanoparticles (negatively charged) of the same core material in an intestinal cell line model [8]. A recent study by Clementino et. al. on the transfer of simvastatin across excised rabbit

nasal mucosa using nanoparticle systems consisting of hybrid lecithin/chitosan (positively charged); polymeric poly- $\epsilon$ -caprolactone stabilized with the nonionic surfactant polysorbate 80 (negatively charged); or polymeric poly- $\epsilon$ -caprolactone stabilized with a polysaccharide-based surfactant (negatively charged) reported an increase in simvastatin transport across the nasal mucosa for the chitosan nanoparticles compared to the other two negatively charged nanoparticles [9]. However, there was about 30% release of simvastatin from the chitosan nanoparticles during the experiment, which may have contributed to its increased transfer. Another study by Chaikhumawang et al. reported an increase in the induction of local and systemic protective response to inactivated PRRSV virus (porcine reproductive and respiratory syndrome virus) loaded in cationic polylactic acid (PLA) nanoparticles when administered intranasally to pigs [10]. However, cationic nanoparticles have also been linked to a variable levels of cellular toxicity [11–15].

In our previous work, we developed polylactic-co-glycolic acid (PLGA) nanoparticles loaded with a fluorescent dye, Nile Red, and tested their uptake across excised bovine nasal mucosa. These negatively charged nanoparticles were able to transfer into the nasal mucosa, and limited uptake was observed with less than 5% of the nanoparticles transferring into the nasal tissues [16]. The investigations of the relationship between nanoparticle characteristics and efficient epithelial uptake are far from complete, and an improved understanding of nano–bio interactions is essential to designing acceptable delivery systems. In this research, we examined the influence of surface charge alteration on the uptake of PLGA nanoparticles across excised nasal mucosal tissues. We especially focused on whether PLGA nanoparticles with a positive surface charge show a different uptake compared to untreated PLGA nanoparticles using excised bovine nasal mucosal tissues.

## 2. Materials and Methods

### 2.1. Materials

PLGA with a 50:50 ratio and 0.32–0.44 dL/g inherent viscosity was obtained from Evonik Industries AG (Darmstadt, Germany). The solvents N,N dimethylformamide (DMF) and acetone were purchased from Fisher Chemicals (Fair Lawn, NJ, USA). Nile Red (5H-Benzo[ $\alpha$ ]phenoxazin-5-one, 9-(diethylamino)), Trypsin-EDTA (0.25%) (with phenol red, and containing no calcium and magnesium), and PAMAM dendrimer (ethylenediamine core, fifth generation (solution, 5 wt.% in methanol) were obtained from MilliporeSigma (St. Louis, MO, USA). Cellosolve<sup>®</sup> Acetate (2-ethoxy ethyl acetate) was obtained from AlfaAesar (Ward Hill, MD, USA). D-Glucose was obtained from Research Products International (RPI) (Mt. Prospect, IL, USA).

### 2.2. Preparation of PLGA Nanoparticles

Unmodified (negatively charged; 60 nm) PLGA nanoparticles were fabricated using a modified surfactant-free nanoprecipitation method that was previously optimized [16]. Briefly, 36 mg of PLGA was dissolved in 5 mL of organic solvent (DMF) in a 15 mL polypropylene tube, and 70  $\mu$ L of fluorescent dye, Nile Red (stock solution 100  $\mu$ g/mL in acetone), was added to the organic phase while vortexing. The polymer and dye solution in DMF (organic phase) was gradually added to Nanopure<sup>®</sup> water (30 mL) (aqueous phase) in a 50 mL glass beaker preheated to 38–40 °C on a heated stirrer plate. The organic phase was added using a 10 mL syringe (without a plunger) connected to a 21G needle that was immersed approximately 1 cm below the water surface while stirring (~300 rpm). The organic phase was poured inside the syringe, and the organic phase left the syringe and entered the aqueous phase due to gravity. After all the organic phase was added into the aqueous phase, the solution was stirred for an additional 2 h, and the temperature was gradually lowered to room temperature (5 °C every 30 min). Dialysis against water (for 35–40 h) was used to remove the organic solvent by placing the nanoparticle dispersion into dialysis tubing (SnakeSkin<sup>®</sup> dialysis tubing with 7000 Da cut-off, Thermo Scientific, Rockford, IL, USA), and the bag was closed and immersed in 4 L of Nanopure<sup>®</sup> Water.

Water was replaced two times during the dialysis period. After dialysis, the nanoparticle dispersion was filtered using 25 µm Whatman<sup>®</sup> filter paper to remove any large aggregates. The nanoparticle dispersion was used to perform the tissue uptake experiment on the same day and any unused dispersion was discarded.

### 2.3. Modification of Surface Charge of 60 nm PLGA Nanoparticles

PLGA nanoparticles with a cationic surface charge were prepared, as discussed in the previous section, with the addition of the PAMAM dendrimer. Fifth generation PAMAM (G5-NH<sub>2</sub> PAMAM) dendrimer solution (15 µL, stock solution 5% *w/w* solution in methanol) was pipetted and mixed with the organic phase (polymer + Nile Red + DMF solvent) prior to the addition to the aqueous phase.

### 2.4. Characterization of Nanoparticles

#### 2.4.1. Dynamic Light Scattering (DLS)

The hydrodynamic diameter and surface charge of the nanoparticles were investigated using a Malvern NanoZS<sup>®</sup> Zetasizer (Malvern Instruments Limited, Worcestershire, UK). One milliliter of nanoparticle dispersion was transferred into a 1 cm acrylic SpectroClear<sup>®</sup> cuvette (Centaur Science, Inc., Stamford, CT, USA). The particle size was measured in backscatter DLS mode. The zeta potential measurements were performed using another 0.8 mL aliquot of nanoparticle dispersion placed in a folded capillary cell (Malvern Instruments Limited, Worcestershire, UK).

#### 2.4.2. Scanning Electron Microscopy (SEM)

Prepared nanoparticles were examined using a Hitachi S4800 electron microscope (Hitachi High Technologies Corporation, Tokyo, Japan) to investigate the nanoparticle size and shape. Diluted nanoparticle dispersion (10 µL of a 1:9 dilution in Nanopure<sup>®</sup> water) was spread on the surface of a silicon chip that was placed on an SEM sample holder. The sample was left to dry in a fume hood, and a thin layer of gold/palladium alloy was used to cover the nanoparticle surface using a sputter coater (Emitech K550, Quorum Technologies Ltd., Kent, UK).

### 2.5. Nile Red Loading and Encapsulation Efficiency

A measured volume of nanoparticle dispersion (1 mL) was diluted 10 times using Nanopure<sup>®</sup> water, and 1 mL was mixed with 1 mL of Cellosolve<sup>®</sup> acetate solvent to extract the loaded dye. The fluorescent dye was quantified in the organic layer by measuring the fluorescent intensity (Ex:520—Ex: 620 nm) with a SpectraMax M5 microplate reader (Molecular Devices, Sunnyvale, CA, USA), and the amount of dye within the nanoparticles was calculated by comparing the measured concentration with a standard curve prepared with known Nile Red concentrations. The amount of the dye in the whole volume of dispersion was determined by comparing the amount in the sample with the total dispersion volume. Nile Red loading was obtained by comparing the measured amount with the amount of Nile Red initially added during the nanoparticle preparation. The percent of encapsulation and loading was calculated using the following equations:

$$\text{Encapsulation Efficiency \%} = \frac{\text{Total amount of dye in the preparation } (\mu\text{g})}{\text{Amount of dye added during preparation } (\mu\text{g})} * 100\% \quad (1)$$

$$\text{Loading } (\mu\text{g of dye per 1 mL of NP dispersion}) = \frac{\text{Amount of dye } (\mu\text{g/mL})}{\text{Amount of NP (mg) per 1 mL of dispersion}} \quad (2)$$

To quantify the amount of nanoparticles in one milliliter, 4 mL samples of three freshly prepared batches of the nanoparticle dispersion were transferred into a pre-weighted 50 mL plastic centrifuge tubes and stored in a  $-80$  freezer for 4 h. Samples were freeze dried using a Labconco freeze dryer (Labconco Corporation, Kansas City, MO, USA). Tubes were weighed again and the average amount of nanoparticle per one milliliter was calculated after subtracting the weight of empty plastic tubes.

#### 2.6. Preparation of Excised Bovine Nasal Tissues

The *in vitro* evaluation of nanoparticle uptake was performed using excised bovine nasal tissues, which have been previously reported to be an acceptable model for the prediction of material transfer across the human nasal mucosa [17]. Bovine nasal tissues were collected from a local abattoir (Buds Meat, Riverside, IA, USA). Collected tissues were kept in 5% *w/v* ice cold glucose solution and kept on ice and transferred back to the laboratory. Nasal mucosa was peeled from the cartilage with a pair of tweezers and mounted on NaviCyte<sup>®</sup> 1 mL vertical diffusion cells (Warner Instruments, LLC, Hamden, CT, USA) with the mucosal surface directed toward the donor side. One milliliter of prewarmed ( $37$  °C) glucose solution (5% *w/v*) was added to the donor and receiver chambers and equilibrated for 10 min at  $37$  °C using a circulating water bath. The diffusion chambers were connected to an oxygen source (Carbogen<sup>®</sup> gas (95% O<sub>2</sub> plus 5% CO<sub>2</sub>) at 3–4 bubbles/sec. This provided mild mixing and maintained tissue aeration. The 5% Glucose *w/v* was shown to be an appropriate equilibration medium instead of a buffer to maintain tissue viability and avoid the aggregation of the nanoparticle suspension which was observed when Krebs–Ringer buffer was mixed with the nanoparticle dispersion [1].

#### 2.7. Nanoparticle Uptake

Glucose powder (equivalent to 5% *w/v*) was added to the dispersion containing the nanoparticles with a mild vortex and pre-warmed ( $37$  °C) in a water bath. After 10 min, the blank glucose solution was removed from the receiver and donor chambers and replaced with 1 mL pre-warmed 5% glucose solution in the receiver chamber and 1 mL of nanoparticle dispersion (containing 5% *w/v* glucose) in the donor chamber. Tissues were incubated with the nanoparticle dispersion for 30 or 60 min. Thereafter, the donor and receiver solutions were collected and transferred into 15 mL polypropylene centrifuge tubes (Sarstedt, Newton, NC, USA). Mucosal tissues were removed from the diffusion cells and rinsed with Nanopure<sup>®</sup> water (3 for 5 s; 3 mL each) to remove surface-attached nanoparticles. The tissue region exposed to the nanoparticles (the exposed area of the vertical diffusion chamber used =  $0.64$  cm<sup>2</sup>) were excised using a curved suture scissor and transferred to a separate 15 mL polypropylene tubes. Trypsin-EDTA solution 0.25% (2 mL) was added to the mucosal tissues to remove the epithelial layer from the submucosal layer, and the tissues were incubated for an additional 2 h. The incubation of the nasal mucosal tissues with trypsin has been shown to effectively separate the epithelial cell layer from the underlying submucosal layer [18,19]. The remaining submucosal tissues were removed from the trypsin solution and were transferred to separate tubes. Cellosolve<sup>®</sup> acetate solvent (1 mL) was pipetted to each tube (receiver solution, epithelial cells in trypsin-EDTA solution, and submucosal tissues) and incubated for >6 h (overnight) to disrupt the tissue, completely dissolve the nanoparticles, and extract the loaded Nile Red dye.

The Nile Red dye was quantified in each tissue layer and the receiver chamber by measuring the fluorescent intensity (Em. 520- Ex. 620 nm) of the sample in Cellosolve<sup>®</sup> acetate using a SpectraMax M5 plate reader (SpectraMax M5, Molecular Devices, Sunnyvale, CA, USA). The amount of nanoparticles transferred into the nasal mucosa was calculated based on the quantified amount of Nile Red (in  $\mu$ g) in each sample and the measured nanoparticle loading ( $\mu$ g of dye per mg of nanoparticles). The amount of nanoparticles was normalized per the surface area ( $\mu$ g of NP per cm<sup>2</sup>) of the mucosal tissues.

### 2.8. Data Analysis

Results were plotted and statistically analyzed using Excel (Microsoft Inc., Redmond, WA, USA) and GraphPad Prism 8 (GraphPad Software, San Diego, CA, USA). A statistically significant p-value was set to be <0.05.

## 3. Results and Discussion

### 3.1. Nanoparticle Characterization

The preparation of unmodified PLGA nanoparticles using the surfactant-free nanoprecipitation method was optimized in our previous study where we showed that this method is reliable, tunable, and reproducible [16]. However, due to the inclusion of a dialysis step against water for a relatively long time, this method may not be optimal for the preparation of nanoparticles loaded with a more hydrophilic cargo molecule than the hydrophobic Nile Red used in these studies.

The PLGA nanoparticles produced using this method showed a unimodal distribution with an average hydrodynamic diameter of 60 nm (polydispersity index = 0.15) and an average zeta potential of  $-28$  mV. Under SEM, the nanoparticles appeared spherical with an average diameter similar to that measured using light scattering.

The Nile Red loading in the PLGA nanoparticles was  $0.60$   $\mu\text{g}/\text{mg}$  of nanoparticles and the encapsulation efficiency was 26% [16]. The encapsulation efficiency of the PAMAM-treated nanoparticles was 23% of the amount of Nile Red originally used during the preparation of the nanoparticle. The loading of Nile was  $0.59$   $\mu\text{g}$  of dye/mg of the PAMAM-PLGA nanoparticles.

The addition of cationic G5-NH<sub>2</sub> PAMAM dendrimers during nanoparticle preparation resulted in the formation of nanoparticles with a positive surface charge and an increase in their hydrodynamic size compared to the PLGA-only nanoparticles. The cationic nanoparticles displayed a unimodal size distribution with a diameter of 103 nm and a heterogeneity index of 0.1 (Figure 1). The zeta potential was slightly positive with an average value of  $+31.4$  mV (Figure 1). The SEM imaging of the cationic nanoparticles showed spherical-shaped particles with an average diameter of between 50–70 nm, which was significantly smaller than the size measurements obtained from dynamic light scattering (Figure 1). This difference is probably due to the presence of the cationic polymer in the formulation, which increases the hydrodynamic diameter of the particles, but the preparation steps for SEM likely condense the PAMAM that may extend from the PLGA nanoparticles surface. Table 1 shows a summary of nanoparticle characteristics used in this study.

**Table 1.** Size and surface charge of PLGA and PAMAM-modified nanoparticles.

Formulation	Average Diameter (by DLS) (nm)	Polydispersity Index (PDI)	Average Zeta Potential (mV)	Nile Red Loading ( $\mu\text{g}/\text{mg}$ )
PLGA nanoparticles	60	0.15	$-28$	0.60
PAMAM Modified PLGA nanoparticles	103	0.1	$+31.4$	0.59

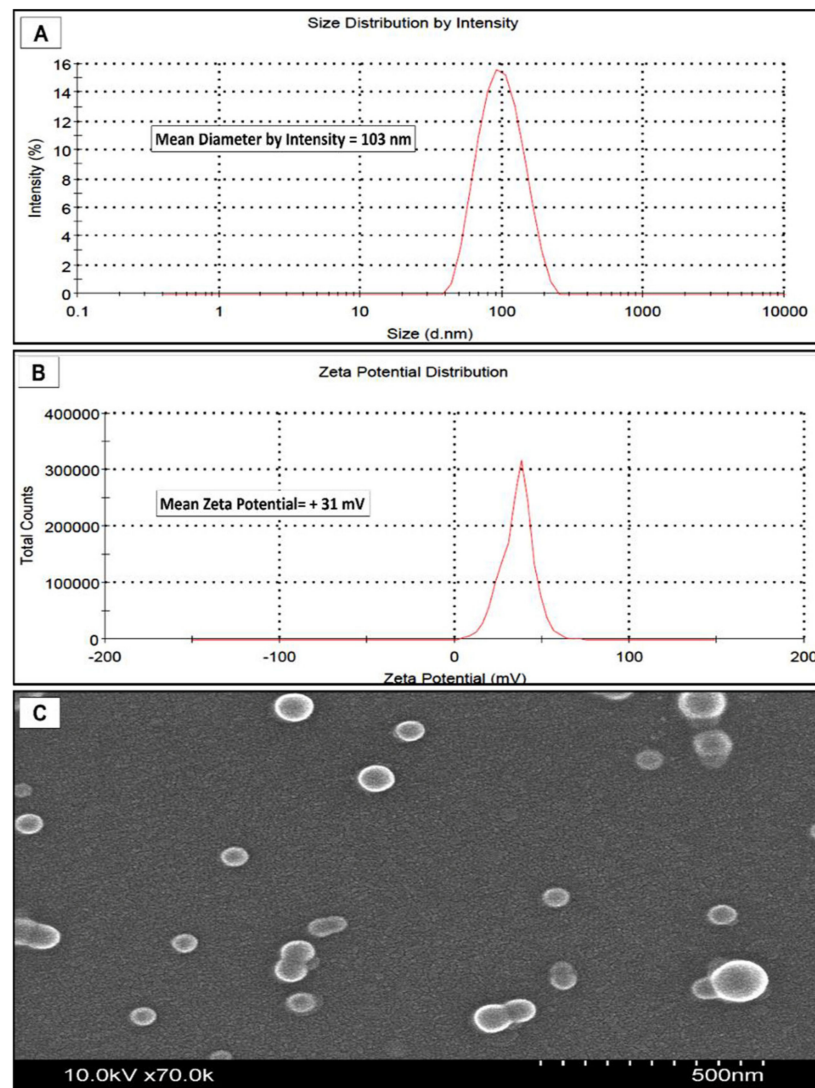


**Figure 1.** Characteristics of positively charged PAMAM-PLGA nanoparticles. (A) DLS measurements of nanoparticle diameter by scattering intensity showing unimodal distribution. (B) Zeta-potential (surface charge) shows a slightly positive surface charge. (C) SEM image shows spherical nanoparticles.

### 3.2. Uptake of Positively Charged PLGA Nanoparticles

Nanoparticle internalization into the excised tissues was previously reported with the polystyrene nanoparticles of various surface charges using fluorescence microscopy in which fluorescence signal was detected at various depths inside the tissue [20]. Cationic nanoparticles were found to transfer into both types of nasal mucosa in as little as 30 min. The uptake was increased with time, and a slightly higher amount of nanoparticle uptake was quantified after 1 h of incubation versus the 30 min incubation period (Figure 2). However, change in time-dependent uptake was not statistically significant in the case of the cationic nanoparticles compared to the previously reported difference observed with unmodified nanoparticles [16]. In those experiments, the PLGA nanoparticles (negatively charged) were transferred into the excised nasal mucosa and a significantly higher amount of nanoparticles was quantified after 60 min of incubation as compared to 30 min of incubation in both respiratory and olfactory mucosae. However, the highest amount transferred was still only about 5% of the amount of nanoparticles originally placed into the donor chamber.

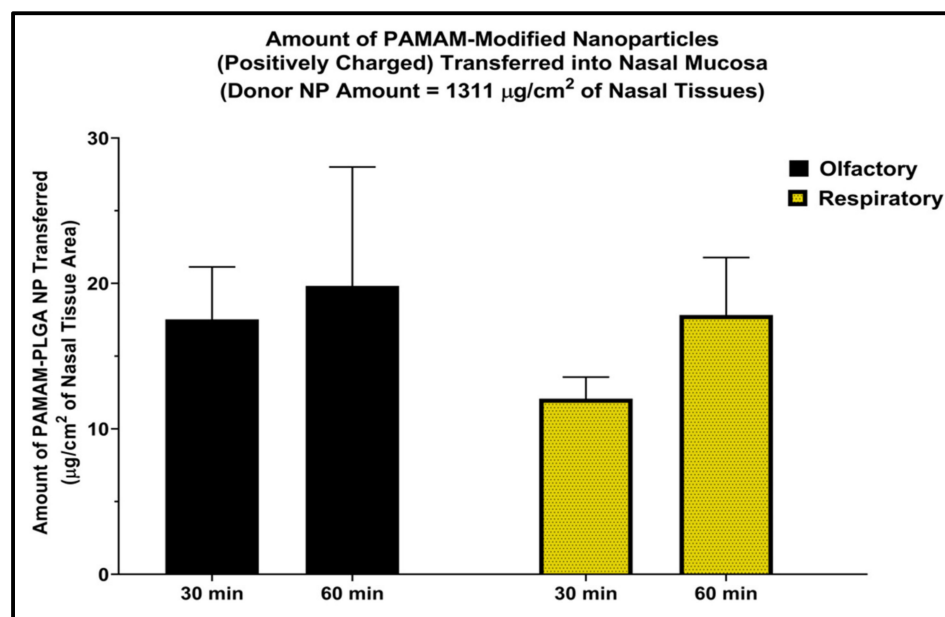


**Figure 2.** Amount of nanoparticles in the nasal mucosa after incubation with PAMAM-modified nanoparticles (cationic PLGA NP) for 30 and 60 min normalized per tissue surface area. The two tailed *t*-test was applied to evaluate the statistical significance.  $n = 3$  each, bars represent mean  $\pm$  SD.

The mean PAMAM-PLGA nanoparticle uptake was no more than 1.5% of the amount of nanoparticles originally placed into the donor chamber. When the cationic nanoparticle uptake was quantified in each tissue layer (epithelial cells and submucosal layer) and the receiver chamber, the amount of nanoparticles quantified in the epithelial cell layer was slightly higher than the amount found in the underlying sub-mucosal layer in both the nasal respiratory and olfactory mucosae, and only a very limited amount of nanoparticles was transferred across the entire nasal mucosa and detected on the receiver media (Figure 3). This demonstrates that the nanoparticles were internalized into the nasal mucosal layers rather than merely being attached to the surface of the tissue. The higher amount of quantified nanoparticles in the epithelial cells shows that this first step in tissue internalization allows for ready (although low efficiency) uptake into the epithelial cells but both PLGA and PAMAM-PLGA nanoparticles transfer more slowly into deeper tissue regions [16].

### 3.3. Effect of Surface Charge Modification on Uptake of 60 nm Nanoparticles

Positively charged nanoparticles showed a significantly reduced uptake into the nasal mucosae compared to unmodified, negatively charged PLGA nanoparticles (Figure 4A,B). The amount of nanoparticles quantified within the mucosal tissues was 1.8–4 times lower when nasal tissues were incubated with PAMAM-containing nanoparticles compared to the amount recovered after incubation with untreated nanoparticles. The electrostatic interactions between the negatively charged cell surface and the positively charged nanoparticles may result in the surface aggregation of the nanoparticles on the cell, and the increased size of these aggregates may hinder their internalization via endocytosis. Previous studies on the uptake of PAMAM-treated PLGA nanoparticles in HEK293 and COS7 cells showed a significant increase in the uptake of cationic nanoparticles in comparison to unmodified particles [21,22], and another study by Bannunah et al. reported a significant increase in the uptake of cationic polystyrene nanoparticles compared with particles with a negative surface charge in Caco-2 and Calu-3 cell line models [8]. However, these studies were performed for longer times (4–16 h), which may suggest longer term changes in nanoparticle uptake mechanisms than were able to be measured in the 1 h incubation conducted on the excised nasal tissues. In addition, nanoparticle uptake may be cell line specific, and cultured cells may not effectively recapitulate the barriers presented by intact nasal tissues,

including the mucus layers and intercellular junctions associated with epithelial tissues. Unfortunately, there is an absence of data comparing nanoparticle uptake by native tissues with uptake in similar tissue-origin cultured cells, and there is not an adequate cell culture model of the human nasal mucosa currently available [1], so while further investigations of nanoparticle uptake in epithelial tissues and in epithelial cell model systems are needed, additional technological advances will need to be made before these additional studies can be conducted.

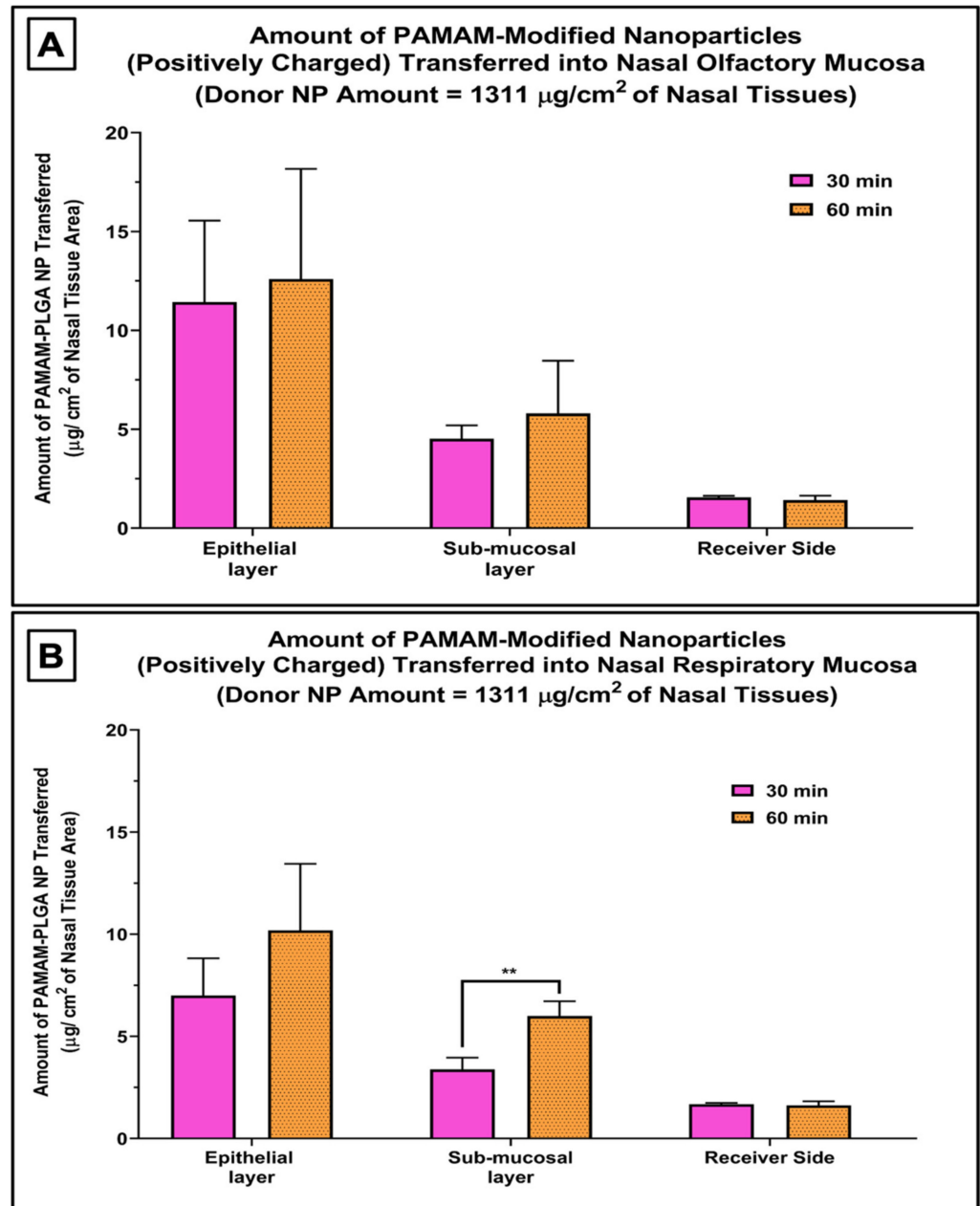


**Figure 3.** Amount of nanoparticles quantified in each mucosal compartment and the receiver media in nasal olfactory mucosa (A), and respiratory mucosa (B) following incubation with the PAMAM-modified nanoparticles (cationic PLGA NP) for 30 and 60 min normalized per tissue surface area. The two tailed t-test was applied to evaluate the statistical significance. Bars are mean  $\pm$  SD. \*\*  $p$ -value = 0.007,  $n$  = 3 each.



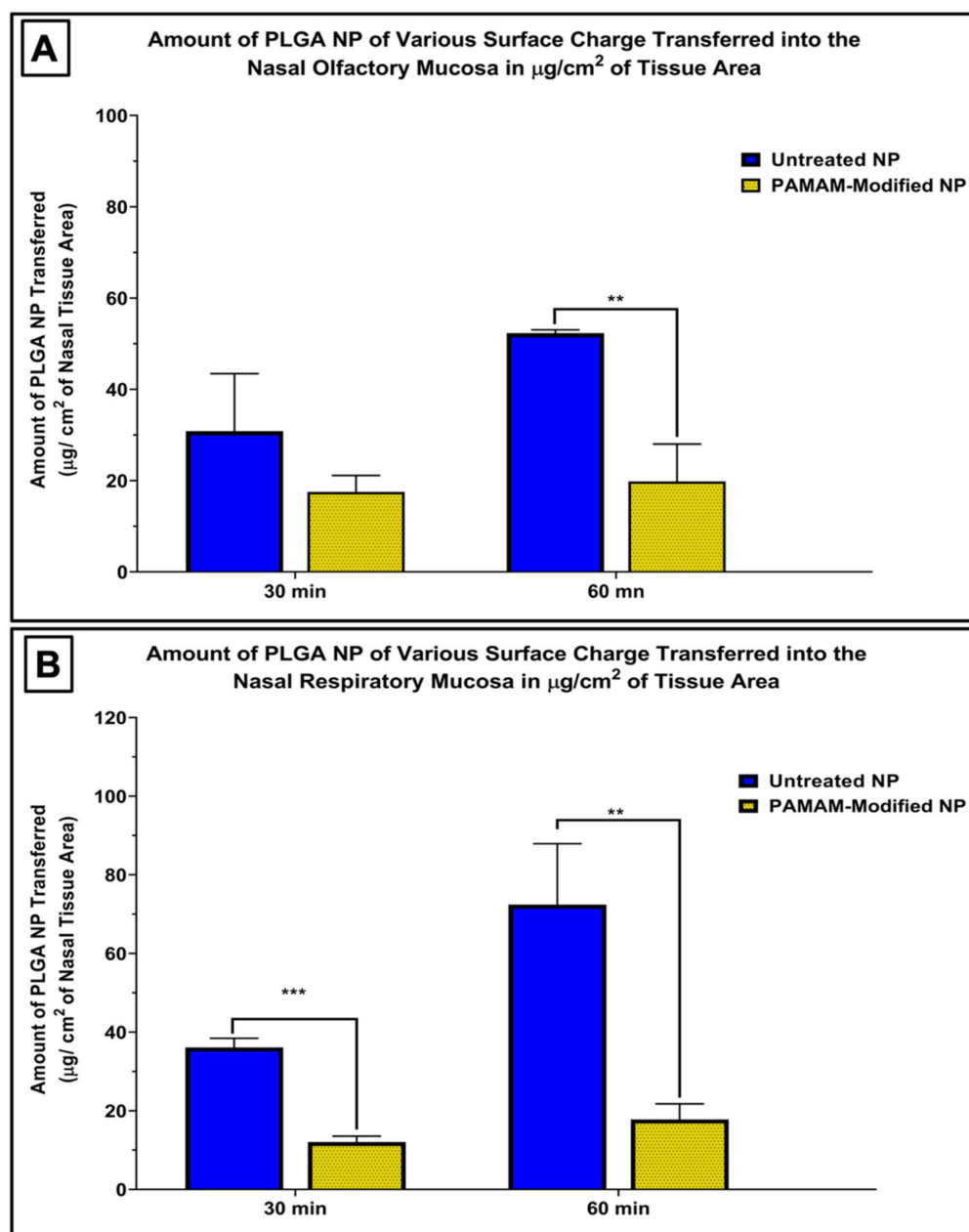


**Figure 4.** Effect of the addition of a polycationic polymer, polyamidoamine dendrimer (5th generation-PAMAM), on the uptake of 60 nm nanoparticles compared to unmodified, negatively charged nanoparticles in the nasal olfactory mucosa (A) and the nasal respiratory mucosa (B) normalized per tissue surface area. Nanoparticle uptake was significantly decreased in both types of mucosae after incubation with PAMAM-modified nanoparticles. The two tailed t-test was applied to evaluate the statistical significance. Bars are mean  $\pm$  SD, bars represent mean  $\pm$  SD, \*\*  $p < 0.005$ ; \*\*\*  $p < 0.001$ ,  $n = 3$  each. Data for untreated nanoparticles were previously reported [16].

PAMAM dendrimers are frequently studied in the delivery of anticancer drugs and gene therapeutics [23]. The PAMAM dendrimer (cationic polymer) has been previously reported to possess some cellular toxicity, and this toxicity is directly related to the generation of the dendrimer, where the 10th generation has a higher toxicity than the 0th generation [24]. The cellular toxicity is reported to occur after a relatively long exposure time (after 24 h of incubation) with the higher generations, and the toxicity was minimal after a short contact time. A study by Intra et al. showed that no significant cytotoxicity was observed when PLGA-PAMAM nanoparticles were incubated with HEK293 cells using the

different generations of dendrimers at different concentrations [21], and these results may indicate that the relative toxicity associated with the inclusion of the PAMAM dendrimer with PLGA nanoparticles in the current work may also be negligible, especially due to the brief incubation time (maximum of 60 min) and low PAMAM generation used (generation 5). If the PAMAM-PLGA nanoparticles were to be further developed as drug delivery systems for human use, additional toxicity evaluations would be needed in light of the potential longer-term exposures that would result from the frequent application of these nanoparticles to the nasal mucosal surface.

#### 4. Conclusions

PAMAM-modified nanoparticles were able to transfer into the excised nasal mucosal tissues within a relatively short time, but the translocation of positively charged nanoparticles was significantly lower when nasal tissues were incubated with the PAMAM-treated nanoparticles (positively charged) compared to unmodified PLGA nanoparticles with a negative surface charge. The differing amounts of nanoparticles present in the nasal respiratory and olfactory mucosae and their epithelial and submucosal regions also suggests the potential for different uptake pathway(s) for the nanoparticles in these different regions of the nasal mucosa. An improved understanding of the particle uptake by epithelial tissues is required to develop optimized nanoparticle-based drug delivery systems for transfer into and across these tissues. Additional investigations evaluating the potential for cellular toxicity after the application of a nanoparticle dispersion or of extracellular drug release from the nanoparticles are also of high importance during the identification of the most promising nanoparticle materials for use in safe and effective nasal delivery systems.

**Author Contributions:** Conceptualization, M.A.A. and M.D.D.; methodology, M.A.A. and M.D.D.; validation, M.A.A.; formal analysis, M.A.A.; investigation, M.A.A.; resources, M.A.A. and M.D.D.; writing—original draft preparation, M.A.A.; writing—review and editing, M.A.A. and M.D.D.; supervision, M.D.D.; project administration, M.A.A. and M.D.D.; funding acquisition, M.D.D. All authors have read and agreed to the published version of the manuscript.

**Funding:** The APC was funded by the corresponding author. Authors also would like to express their thankfulness to the Al-Mustaqbal University College, Babylon, Iraq, for the support provided to accomplish this report (grant number MUC-M-0222).

**Institutional Review Board Statement:** Not applicable.

**Informed Consent Statement:** Not applicable.

**Data Availability Statement:** All data are included within the article.

**Conflicts of Interest:** The authors declare no conflict of interest.

#### References

1. Albarki, M. Evaluation of poly D, L Lactic-co-glycolic Acid (PLGA) Nanoparticle Uptake Pathways Across the Nasal Mucosa. Ph.D. Thesis, University of Iowa, Iowa City, IA, USA, 2019. [[CrossRef](#)]
2. Al Khafaji, A.S.; Donovan, M.D. Endocytic Uptake of Solid Lipid Nanoparticles by the Nasal Mucosa. *Pharmaceutics* **2021**, *13*, 761. [[CrossRef](#)] [[PubMed](#)]
3. Peer, D.; Karp, J.M.; Hong, S.; Farokhzad, O.C.; Margalit, R.; Langer, R. Nanocarriers as an emerging platform for cancer therapy. *Nat. Nanotechnol.* **2007**, *2*, 751–760. [[CrossRef](#)]
4. Albanese, A.; Tang, P.S.; Chan, W.C.W. The Effect of Nanoparticle Size, Shape, and Surface Chemistry on Biological Systems. *Annu. Rev. Biomed. Eng.* **2012**, *14*, 1–16. [[CrossRef](#)] [[PubMed](#)]
5. Du, B.; Yu, M.; Zheng, J. Transport and interactions of nanoparticles in the kidneys. *Nat. Rev. Mater.* **2018**, *3*, 358–374. [[CrossRef](#)]
6. Choi, H.S.; Liu, W.; Liu, F.; Nasr, K.; Misra, P.; Bawendi, M.G.; Frangioni, J.V. Design considerations for tumour-targeted nanoparticles. *Nat. Nanotechnol.* **2009**, *5*, 42–47. [[CrossRef](#)] [[PubMed](#)]
7. Decuzzi, P.; Godin, B.; Tanaka, T.; Lee, S.-Y.; Chiappini, C.; Liu, X.; Ferrari, M. Size and shape effects in the biodistribution of intravascularly injected particles. *J. Control. Release* **2010**, *141*, 320–327. [[CrossRef](#)]
8. Bannunah, A.M.; Vllasaliu, D.; Lord, J.; Stolnik, S. Mechanisms of Nanoparticle Internalization and Transport Across an Intestinal Epithelial Cell Model: Effect of Size and Surface Charge. *Mol. Pharm.* **2014**, *11*, 4363–4373. [[CrossRef](#)] [[PubMed](#)]

9. Clementino, A.R.; Pellegrini, G.; Banella, S.; Colombo, G.; Cantù, L.; Sonvico, F.; Del Favero, E. Structure and Fate of Nanoparticles Designed for the Nasal Delivery of Poorly Soluble Drugs. *Mol. Pharm.* **2021**, *18*, 3132–3146. [[CrossRef](#)] [[PubMed](#)]
10. Chaikhumwang, P.; Madapong, A.; Saeng-Chuto, K.; Nilubol, D.; Tantituvanont, A. Intranasal delivery of inactivated PRRSV loaded cationic nanoparticles coupled with enterotoxin subunit B induces PRRSV-specific immune responses in pigs. *Sci. Rep.* **2022**, *12*, 3725. [[CrossRef](#)]
11. McNeil, S.E. Nanoparticle Therapeutics: A Personal Perspective. *Wiley Interdiscip. Rev. Nanomed. Nanobiotechnol.* **2009**, *1*, 264–271. [[CrossRef](#)]
12. Goodman, C.M.; McCusker, C.D.; Yilmaz, A.T.; Rotello, V.M. Toxicity of Gold Nanoparticles Functionalized with Cationic and Anionic Side Chains. *Bioconjug. Chem.* **2004**, *15*, 897–900. [[CrossRef](#)] [[PubMed](#)]
13. Leroueil, P.R.; Berry, S.A.; Duthie, K.; Han, G.; Rotello, V.M.; McNerny, D.Q.; Baker, J.R., Jr.; Orr, B.G.; Holl, M.M.B. Wide Varieties of Cationic Nanoparticles Induce Defects in Supported Lipid Bilayers. *Nano Lett.* **2008**, *8*, 420–424. [[CrossRef](#)]
14. Verma, A.; Uzun, O.; Hu, Y.; Hu, Y.; Han, H.-S.; Watson, N.; Chen, S.; Irvine, D.J.; Stellacci, F. Surface-structure-regulated cell-membrane penetration by monolayer-protected nanoparticles. *Nat. Mater.* **2008**, *7*, 588–595. [[CrossRef](#)] [[PubMed](#)]
15. Dobrovolskaia, M.A.; McNeil, S.E. Immunological properties of engineered nanomaterials. *Nat. Nanotechnol.* **2007**, *2*, 469–478. [[CrossRef](#)]
16. Albarki, M.A.; Donovan, M.D. Bigger or Smaller? Size and Loading Effects on Nanoparticle Uptake Efficiency in the Nasal Mucosa. *AAPS PharmSciTech* **2020**, *21*, 1–8. [[CrossRef](#)]
17. Schmidt, M.C.; Simmen, D.; Hilbe, M.; Boderke, P.; Ditzinger, G.; Sandow, J.; Lang, S.; Rubas, W.; Merkle, H.P. Validation of Excised Bovine Nasal Mucosa as in vitro Model to Study Drug Transport and Metabolic Pathways in Nasal Epithelium. *J. Pharm. Sci.* **2000**, *89*, 396–407. [[CrossRef](#)]
18. Al Bakri, W.S.H. Characterization of Atrazine Transport Across Nasal Respiratory and Olfactory Mucosa. Master's Thesis, The University of Iowa, Iowa City, IA, USA, 2014. [[CrossRef](#)]
19. Chen, N. Size and Surface Properties Determining Nanoparticle Uptake and Transport in the Nasal Mucosa. Ph.D. Thesis, The University of Iowa, Iowa City, IA, USA, 2013. [[CrossRef](#)]
20. Mistry, A.; Stolnik, S.; Illum, L. Nose-to-Brain Delivery: Investigation of the Transport of Nanoparticles with Different Surface Characteristics and Sizes in Excised Porcine Olfactory Epithelium. *Mol. Pharm.* **2015**, *12*, 2755–2766. [[CrossRef](#)] [[PubMed](#)]
21. Intra, J.; Salem, A.K. Fabrication, Characterization and In Vitro Evaluation of poly (D,L-lactide-co-glycolide) Microparticles Loaded with Polyamidoamine-Plasmid DNA Dendriplexes for Applications in non-viral Gene Delivery. *J. Pharm. Sci.* **2010**, *99*, 368–384. [[CrossRef](#)]
22. Zhang, X.-Q.; Intra, J.; Salem, A.K. Conjugation of Polyamidoamine Dendrimers on Biodegradable Microparticles for Nonviral Gene Delivery. *Bioconjug. Chem.* **2007**, *18*, 2068–2076. [[CrossRef](#)] [[PubMed](#)]
23. Surekha, B.; Kommana, N.S.; Dubey, S.K.; Kumar, A.P.; Shukla, R.; Kesharwani, P. PAMAM dendrimer as a talented multi-functional biomimetic nanocarrier for cancer diagnosis and therapy. *Colloids Surf. B Biointerfaces* **2021**, *204*, 111837. [[CrossRef](#)] [[PubMed](#)]
24. Harper, S.; Pryor, J.; Harper, B. Comparative toxicological assessment of PAMAM and thiophosphoryl dendrimers using embryonic zebrafish. *Int. J. Nanomed.* **2014**, *9*, 1947–1956. [[CrossRef](#)] [[PubMed](#)]